Q/V-Band Planar Array Antenna integrated with a Low-cost 3D Printed Dielectric Polarizer and lens

Hakmin Lee
Satellite Payload Research Section
Electronics and Telecommunications
Research Institute
Daejeon, Republic of Korea
hakhak@etri.re.kr

Seong-Mo Moon
Satellite Payload Research Section
Electronics and Telecommunications
Research Institute
Daejeon, Republic of Korea
smmoon @etri.re.kr

Dongpil Chang
Satellite Payload Research Section
Electronics and Telecommunications
Research Institute
Daejeon, Republic of Korea
dpjang@etri.re.kr

Abstract—This paper presents a novel circularly polarized antenna system for Q/V-band LEO satellite communications that integrates a microstrip patch antenna with a dielectric polarizer, cross-slot, and hemispherical lens. The key innovation is the dielectric cross-slot that simultaneously improves impedance matching and stabilizes axial ratio below 3 dB across the operating band. The single-element achieves 18.43 dBic peak gain with over 14.76 dB XPD, while the 1×5 array naturally generates multi-beam patterns with $\pm 22^{\circ}$ steering capability due to differential focal lengths. This design eliminates complex feeding networks while providing cost-effective mass production for LEO constellation deployments.

Keywords— LEO satellite communication, Dielectric polarizer, Dielectric lens antenna

I. INTRODUCTION

In the rapidly evolving satellite communication landscape, the demand for Q/V-band frequencies (33-75GHz) has significantly increased due to the saturation of traditional Ku/Ka-band spectrum resources. This frequency shortage has driven the industry toward exploring higher frequency bands that offer wider bandwidth and enhanced data transmission capabilities for next-generation communication systems. Low Earth Orbit (LEO) satellite constellations, operating with hundreds to thousands of satellites, have emerged as a dominant architecture for global broadband coverage, necessitating the development of low-cost satellite payload components to achieve economic viability [1]-[3]. The substantial distance between LEO satellites and ground stations, combined with orbital dynamics and atmospheric effects, makes precise antenna alignment extremely challenging, thus requiring circularly polarized (CP) antennas to eliminate polarization mismatch losses inherent in linearly Conventional approaches systems. implementing CP in planar array antennas typically employ either individual CP radiating elements or sequential feeding networks with 90° phase differences between adjacent ports. However, these methods introduce significant design complexity, requiring precise phase control circuits, multiple feeding layers, or sophisticated element geometries that become increasingly sensitive to fabrication tolerances at Q/V-band frequencies. The manufacturing precision required for such high-frequency implementations often results in substantial performance degradation and increased production costs, making them unsuitable for large-scale LEO constellation deployment. Consequently, developing a simplified yet high-performance CP antenna solution suitable

for cost-effective mass production has become essential for LEO satellite communication applications [4]-[6].

II. PROPOSED SINGLE ANTENNA

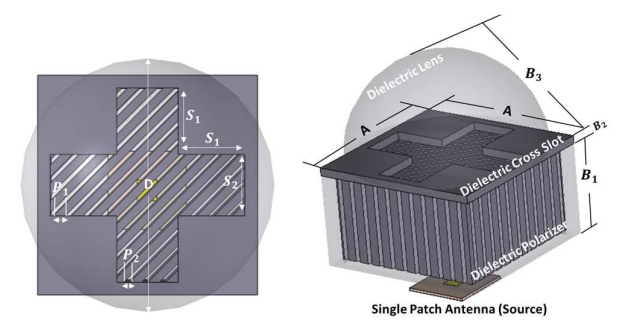


Fig. 1. Configurations of proposed antenna with dielectric polaizer and lens

The proposed antenna system consists of a microstrip patch antenna integrated with a dielectric polarizer, a dielectric cross-slot, and a hemispherical dielectric lens. The patch antenna is fabricated on a Rogers 5880 substrate with a dielectric constant of 2.2, a loss tangent of 0.0009, and a thickness of 0.254 mm. To achieve circular polarization and improve axial ratio (AR) performance, a dielectric polarizer is co-designed with the antenna feed. Between the polarizer and the lens, a dielectric cross-slot structure is introduced, which plays a crucial role in simultaneously matching the impedance and axial ratio by introducing additional resonances and enabling more efficient polarization conversion. The dielectric polarizer, cross-slot, and lens are all realized with the same dielectric material, having a dielectric constant of 2.9 and a dissipation factor of 0.01, which simplifies fabrication and ensures consistent electromagnetic behavior across the entire structure. The operating principle of the dielectric polarizer can be explained by its ability to introduce a 90° phase delay between orthogonal field components, thereby converting linearly polarized waves from the patch antenna into circularly polarized waves. Such dielectric polarizers are widely used in high-gain circularly polarized antenna systems and can be realized with low-cost fabrication techniques. Finally, the hemispherical dielectric lens is employed to further enhance the gain and directivity of the antenna system by focusing the radiated fields from the patch-polarizer structure, improving boresight gain while maintaining a stable axial ratio bandwidth.

TABLE I. Dimensions of the Proposed Antenna Element (Unit: λ_n @ $50\mathrm{GHz}$)

S_1	S_2	P_1	P_2	B_1	B_2	B_3
1.04	0.81	0.16	0.08	1.45	0.13	2.35
A	D	d	A'	В'	D'	L
2.71	3.33	0.42	4.46	4.37	4.37	2.67

This integrated antenna system, combining the patch antenna, dielectric polarizer, cross-slot, and hemispherical lens, constitutes the complete proposed antenna design. In this configuration, the synergistic interaction among the polarizer, cross-slot, and lens not only yields improved reflection coefficient and axial ratio performance but also enables the possibility of reducing the physical size of the dielectric polarizer and lens without sacrificing efficiency.

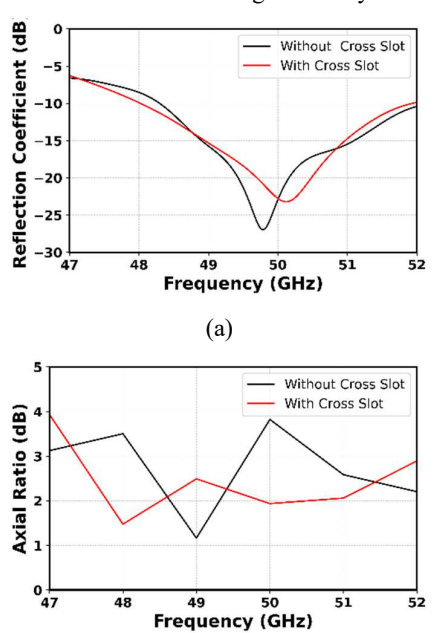


Fig. 2. Comparison of simulated reflection coefficient and axial ratio (AR) of the proposed antenna with and without a dielectric cross-slot.

Fig. 2 Simulated reflection coefficient and axial ratio (AR) of the proposed antenna composed of the source patch antenna, dielectric polarizer, dielectric cross-slot, and hemispherical dielectric lens, comparing the configurations with and without the dielectric cross-slot between the polarizer and the lens. The performance comparison is based on the identical structural dimensions summarized in Table 1. Regarding the reflection coefficient, the configuration without the cross-slot achieves an impedance bandwidth of 48.3–52.0 GHz (7.3%), whereas the configuration with the cross-slot extends the bandwidth to 48.0-51.94 GHz (7.9%), showing a clear improvement in impedance matching. For axial ratio performance, the configuration without the cross-slot shows regions exceeding 3 dB within the operating band due to phase distortion between orthogonal field components. In contrast, with the cross-slot, the AR remains below 3 dB across the entire operating band, demonstrating that the cross-slot

effectively compensates for phase errors and stabilizes CP performance. This enhancement is attributed to the cross-slot introducing an additional resonance that optimizes the electromagnetic field distribution and enabling improved coupling between the dielectric medium and surrounding air interface, thereby facilitating more efficient polarization conversion and phase matching between orthogonal field components. Fig. 3 presents the simulated beam patterns of the proposed antenna, which includes the dielectric polarizer, dielectric cross-slot, and hemispherical dielectric lens. For the $\varphi = 0^{\circ}$ cut, the co-polarization (LHCP) gain is 18.35 dBic, while the cross-polarization (RHCP) level is 3.59 dBic, yielding a cross-polarization discrimination (XPD) of 14.76 dB. For the $\varphi = 90^{\circ}$ cut, the co-polarization (LHCP) gain is 18.43 dBic and the cross-polarization (RHCP) level is 0.29 dBic, resulting in an XPD of 18.14 dB. These results verify that the dielectric cross-slot improves both AR and impedance matching, thereby allowing further reduction of the dielectric polarizer and hemispherical lens dimensions without sacrificing performance. Moreover, the incorporation of the polarizer and cross-slot preserves the radiation characteristics, showing consistency with those obtained when employing the dielectric lens alone.

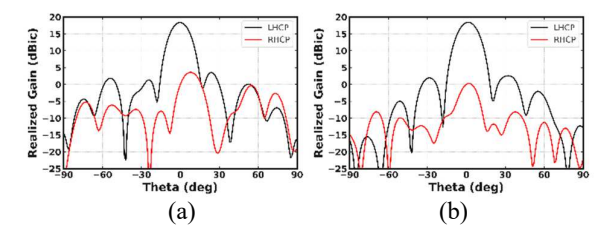


Fig. 3. Simulated radiation patterns of the proposed antenna: (a) ϕ = 0° cut, (b) ϕ = 90° cut.

III. PROPOSED 1X5 ARRAY ANTENNA BY DESCRIPTION AI AI AI AI AI Array Patch Antenna (Source)

Fig. 4. Configurations of proposed 1x5 array antenna.

The final configuration extends the single-element design to a 1×5 array antenna, as shown in Fig. 4. The array is composed of five patch antenna sources, a dielectric polarizer, a dielectric cross-slot, and a hemispherical dielectric lens. The overall dimensions of the structure are defined by five design parameters, indicated in Fig. 4 and summarized in Table 1. The distance between elements in the array is defined as *d*. Unlike conventional arrays that combine multiple sources into a single beam, this design enables each element to radiate an independent beam. This phenomenon occurs because the spacing d between array elements and the lens results in different effective focal lengths for each source. As a result, each source radiates a beam in a different direction, and the array naturally produces a multi-beam radiation pattern [7]. This property is highly attractive for LEO satellite

constellation applications, where simultaneous multi-user coverage and efficient spectrum reuse are required.

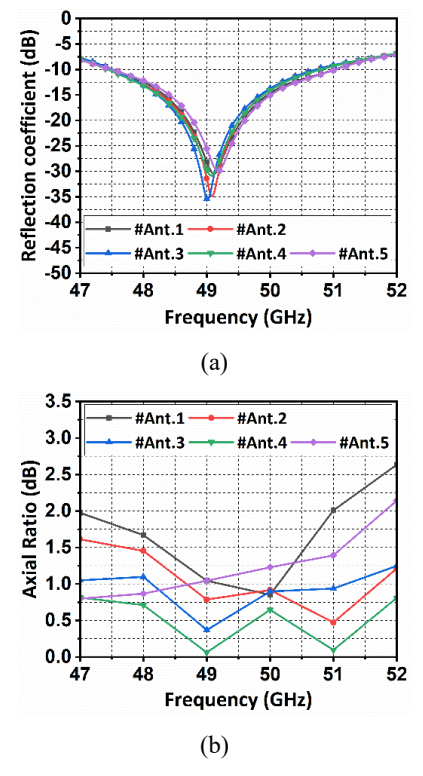


Fig. 5. Simulated reflection coefficient and axial ratio (AR) of the proposed array antenna.

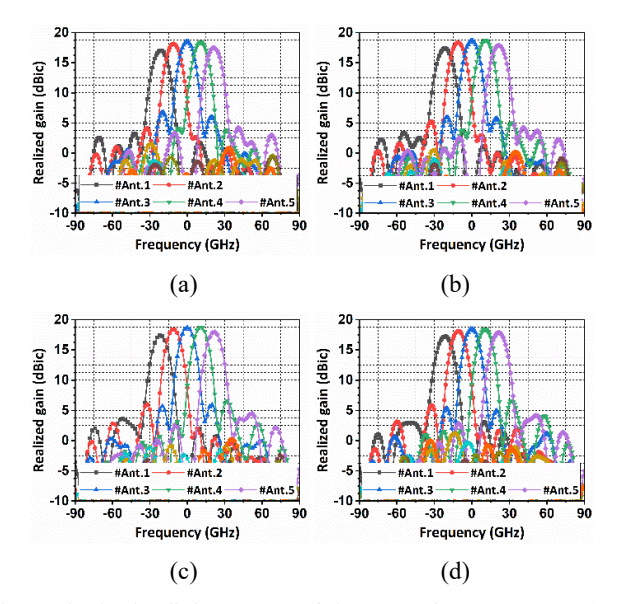


Fig. 6. Simulated radiation patterns of the proposed array antenna: (a) 48GHz, (b) 49GHz, (c) 50GHz, (d) 51GHz.

The Fig. 5 presents the simulated reflection coefficient and axial ratio (AR) of the proposed 1×5 array antenna. The reflection coefficient shows an impedance bandwidth of 47.515–50.720 GHz, corresponding to 3.205 GHz or 6.53% with respect to the center frequency of 49.118 GHz. In addition, the AR remains below 3 dB across the entire operating band for all five antenna elements, confirming stable

circular polarization. Fig. 6 illustrates the radiation patterns of the array at representative frequencies, where only the result at the center frequency of 49 GHz is discussed. At this frequency, the central element (Ant#3) achieves a peak gain of 18.71 dBic at $\theta=0^{\circ}$, while the other elements steer beams toward $\theta=-22^{\circ},-11^{\circ},+11^{\circ},$ and $+22^{\circ}$ with peak gains ranging from 17.41 dBic to 18.80 dBic. The lowest XPD among the five elements is approximately 24 dB, which is sufficient to ensure high polarization purity and stable CP radiation. These results verify that the proposed 1×5 array antenna achieves wideband impedance matching, stable AR, and high-gain multi-beam radiation, making it highly suitable for LEO satellite communication systems.

IV. CONCLUSION

This work demonstrates a cost-effective circularly polarized antenna for Q/V-band LEO satellites, addressing spectrum scarcity and polarization mismatch. The dielectric cross-slot integration enhances impedance matching and axial ratio, while enabling natural multi-beam generation without complex feeding networks. With peak gains above 18 dBic, stable circular polarization, and simplified manufacturing using uniform dielectric materials, the design advances mass deployment of next-generation LEO constellations for global broadband coverage.

ACKNOWLEDGMENT

This work was supported by a grant from the Institute of Information & Communications Technology Planning & Evaluation (IITP), funded by the Korean government (MSIT) (No. 2021-0-00847, Development of core technologies for 3D Coverage Satellite Communication).

This work was supported by a grant from the Institute of Information & Communications Technology Planning & Evaluation (IITP), funded by the Korean government (MSIT) (No. 2018-0- 00190, Development of Core Technology for Satellite Payload).

REFERENCES

- [1] O. Kodheli *et al.*, "Satellite Communications in the New Space Era: A Survey and Future Challenges," in *IEEE Communications Surveys & Tutorials*, vol. 23, no. 1, pp. 70-109, Firstquarter 2021.
- [2] B. Al Homssi et al., "Next Generation Mega Satellite Networks for Access Equality: Opportunities, Challenges, and Performance," in *IEEE Communications Magazine*, vol. 60, no. 4, pp. 18-24, April 2022
- [3] G. Iacovelli, C. Lacoste, E. Lagunas and S. Chatzinotas, "Ground Segment Design for Q/V Band NGSO Satellite Systems via ℓ₀-Norm Minimization," in *IEEE Wireless Communications Letters*, vol. 14, no. 3, pp. 756-760, March 2025.
- [4] Al-Alem, Y., Sifat, S.M., Antar, Y.M.M. et al. Millimeter-wave planar antenna array augmented with a low-cost 3D printed dielectric polarizer for sensing and internet of things (IoT) applications. Sci Rep 13, 9646 (2023).
- [5] R. J. Zhu et al., "3-D Printed Planar Dielectric Linear-to-Circular Polarization Conversion and Beam-Shaping Lenses Using Coding Polarizer," in *IEEE Transactions on Antennas and Propagation*, vol. 68, no. 6, pp. 4332-4343, June 2020.
- [6] K. X. Wang and H. Wong, "Design of a Wideband Circularly Polarized Millimeter-Wave Antenna With an Extended Hemispherical Lens," in *IEEE Transactions on Antennas and Propagation*, vol. 66, no. 8, pp. 4303-4308, Aug. 2018.
- [7] D. F. Filipovic, G. P. Gauthier, S. Raman and G. M. Rebeiz, "Off-axis properties of silicon and quartz dielectric lens antennas," in *IEEE Transactions on Antennas and Propagation*, vol. 45, no. 5, pp. 760-766, May 1997.